

## Physicochemical and crystalline properties of standard maize starch hydrothermally treated by direct steaming



Seyed-Amir Bahrani<sup>a,b</sup>, Catherine loisel<sup>c</sup>, Sid-Ahmed Rezzoug<sup>a</sup>, Stéphane Cohendoz<sup>a</sup>, Alain Buleon<sup>d</sup>, Zoulikha Maache-Rezzoug<sup>a,\*</sup>

<sup>a</sup> LaSIE, Université de La Rochelle, UMR-CNRS 7356, France

<sup>b</sup> Université Paris Diderot, Sorbonne Paris Cité, MSC, UMR 7057, CNRS, F-75013, Paris, France

<sup>c</sup> LUNAM Université, ONIRIS, CNRS, GEPEA, UMR 6144, Site de la Géraudière, Nantes F-44322, France

<sup>d</sup> INRA – Biopolymères Interactions Assemblages (UR1268), F-44300 Nantes, France

### ARTICLE INFO

#### Article history:

Received 22 June 2016

Received in revised form 4 October 2016

Accepted 5 October 2016

Available online 5 October 2016

#### Keywords:

Standard maize starch

Hydrothermal processes

Physicochemical properties

Particle aggregation

### ABSTRACT

The changes in physicochemical properties of standard maize starch (SMS) by three hydrothermal treatments; DV-HMT (Direct Vapor-Heat Moisture Treatment), RP-HMT (Reduced Pressurized-Heat Moisture Treatment) and DIC (instantaneous controlled pressure drop) were investigated at different processing conditions; steam pressure (SP) varied from 1 to 3 bar during 20 min. Starch was steamed by direct contact, whose interest was to intensify the heat transfer phenomenon but also the water transfer. The physicochemical changes of SMS depended on process conditions and their extent followed this order: DIC > RP-HMT > DV-HMT. All treatments significantly increased gelatinization temperatures and decreased the enthalpies, confirmed by loss of granules birefringence. From 2 bar, the crystalline structure changed from A-type to V<sub>h</sub>-type, revealing formation of amylose-lipid complexes during steaming. The results clearly showed that the particle size distribution depends on the melting extent of crystalline structure during treatment. At severe processing conditions the melted fraction increased and more complex aggregates of different sizes have been formed.

© 2016 Published by Elsevier Ltd.

### 1. Introduction

Starch which is a renewable biopolymer and one of the most abundant carbohydrates reserve, constitutes a fundamental material for food and non-food use due to its large physicochemical properties. Generally, modification of starch is carried out to enhance the positive characteristics and eliminate the shortcomings of native starches. Heat-Moisture Treatment (HMT) modifies the physicochemical properties of starch without destroying the granular structure. Starch is heated at high temperature (<140 °C) but with restricted moisture between 13 and 30 g/100 g (Arns et al., 2015; Kong et al., 2014; Sui et al., 2015; Zen, Ma, Kong, Gao, & Yu, 2015), above its glass transition temperature and below the gelatinization temperature for times of few minutes (Zarguili, Maache-Rezzoug, Loisel, & Doublier, 2006; Lim, Chang, & Chung, 2001) to hours (Ji et al., 2015; Kong et al., 2014; Wang, Zhang, Chen, & Li, 2016). The comprehension of starch phase transitions is extremely important in the food processing operations. Starch with

a semi-crystalline structure has two phase transitions which are likely to occur during HMT treatment: the glass transition that concerns the amorphous phase (mainly the branching regions of the amylopectin and most of amylose chains) and melting of crystallites (formed by adjacent short chains of amylopectin intertwined into double helices). The melting temperatures of crystallites depend strongly on the moisture content. For moisture content higher than 60% (w/w), only one single endotherm occurs over a constant temperature range, reflecting the loss of semi-crystalline order and transition temperature is referred to as gelatinization temperature. For lower moisture contents, multiple transitions occur that reflect melting and recrystallisation processes appearing simultaneously during heating (Biliaderis, Page, Maurice, & Juliano, 1986; Maache-Rezzoug, Zarguili, Loisel, Queveau, & Buleon, 2008). The transition temperatures, designated as melting temperatures, increase and multiple endotherms are formed to the detriment of gelatinization endotherm. The melting term is then preferred to describe the thermal transitions during heating at low or intermediate moisture contents. In a previous work (Maache-Rezzoug et al., 2008), we have shown that the low moisture content (i.e. less than 35%) prevailing during DIC treatment were not sufficient to ensure that the gelatinisation happens. Many studies have been carried out

\* Corresponding author.

E-mail address: [zrezzoug@univ-lr.fr](mailto:zrezzoug@univ-lr.fr) (Z. Maache-Rezzoug).

on physicochemical properties of starch granules after HMT treatment. The properties of treated starches depend on the starch origin (Maache-Rezzoug, Zarguili, Loisel, & Doublier, 2010; Collado, & Corke, 1999; Gunaratne, & Hoover, 2002; Hoover and Manuel, 1996; Hoover and Vasanthan, 1994; Kulp, & Lorenz, 1981) and treatment conditions used (Kong et al., 2014; Sui et al., 2015; Takaya and Nishinari, 2000).

Some investigations (Chung, Liu, & Hoover, 2009; Gunaratne, & Hoover, 2002; Hoover & Manuel, 1996; Malumba, Massaux, Deroanne, Masimango, & Bera, 2009; Vermeylen, Goderis, Reynaers, & Delcour, 2006) have shown that the characteristic temperatures and enthalpy of gelatinization ( $\Delta H$ ) of treated starches by HMT were mainly influenced by applied moisture level and temperature. Maache-Rezzoug, Zarguili, Loisel, Doublier, & Buléon (2011) observed similar effects after DIC treatment, except that the gelatinization temperature range was narrowed as observed with annealing (Hublin, 1994; Jayakody & Hoover, 2008). The authors suppose that the DIC treatment has led first the melting of crystallites of low cohesion, those requiring less energy and the remaining crystallites in the residual structure have greater cohesion. Bahrani, Loisel, Doublier, Rezzoug, & Maache-Rezzoug (2012) have already shown during the steaming of SMS by three HMT processes that the heating of starch granules is the result of transfer of latent heat of steam condensation by direct contact with saturated steam that also contributed to water transfer. Starch temperature rises from room temperature to steam equilibrium temperature. The higher the difference in temperature, the higher the quantity of condensed water, which causes increasing of starch moisture content (Zarguili et al., 2006). Direct Vapour-Heat Moisture Treatment, termed as DV-HMT treatment by our team, consists in heating up starch by saturated steam injected from atmospheric pressure up to processing steam pressure level. This treatment belongs to HMT according to the definition of Sair and Fetzer (1944). As regards to RP-HMT (Maruta et al., 1994) and DIC, the two processes begin by the setting up of vacuum prior to injection of saturated steam, contributing to intensify its diffusion into the product by reducing the air resistance. Consequently, the time required to reach steam equilibrium temperature is shortcut (Bahrani, Monteau, Rezzoug, Loisel, & Maache-Rezzoug, 2014). Only DIC process contains a final step of abrupt decompression which carries out towards the vacuum (Rezzoug, Maache-Rezzoug, Mazoyer, & Allaf, 2000) instead of atmospheric pressure as for DV-HMT and RP-HMT. When pressure suddenly decreases, the autovaporization which is an adiabatic transition occurs and water rashly escapes accompanied by a rapid cooling, whose value stabilizes at the equilibrium temperature of final pressure. The mechanical action and the intense shear of granules contribute to alter the crystalline structure; some mechanical energy is converted into internal energy (Huang, Lu, Li, & Tong, 2007). Bahrani et al. (2014) and Zarguili, Maache-Rezzoug, Loisel and Doublier (2009) showed during DV-HMT and RP-HMT/DIC processes that the treatments were homogeneous; the absence of moisture gradients between the different starch layers was evidenced during monitoring of spatial evolution of moisture content in the thickness direction at different processing times. The presence of initial vacuum in the case of RP-HMT/DIC, contributes to generate a more significant amount of condensed steam than for DV-HMT, the moisture content were 24 and 20%, respectively. For a same SP, the volume occupied by air in the reactor is replaced by an equivalent volume of steam. The objective of this study was to investigate the effect of three hydrothermal processes; DV-HMT RP-HMT and DIC on the physicochemical changes of SMS. The impact of processes, mainly the additional vacuum steps before and after steaming phase of starch granules, on the thermal transitions, structural characteristics and morphological properties were investigated at different processing temperatures.

## 2. Materials and methods

### 2.1. Raw material

Standard maize starch (SMS) at residual moisture content of 14% (g H<sub>2</sub>O/g db) and with relative weight percentages of amylose and amylopectin of 26 and 74%, respectively, was supplied by Roquette Frères (Lestrem, France).

### 2.2. Moisture content measurement

Moisture content was determined by air oven at 105 °C during 3 h, according to the A.O.A.C (1999) standard method. As the evaporation phenomenon during the pressure release can disturb the real estimation of absorbed water, the brutal decompression of DIC was replaced by a gradual depressurization to atmospheric pressure and thus the moisture content in RP-HMT and DIC are similar. Three replicates were performed and the standard deviation was about 0.2% (dry basis).

### 2.3. Experimental set-up

The detailed procedure and equipment have been described previously by Bahrani, Loisel, Maache-Rezzoug, Della Valle, & Rezzoug (2013). Briefly, the experimental setup is composed from: a processing reactor, where the sample was treated at high SP/temperature, a vacuum system which comprises mainly a stainless steel vacuum tank with a volume of 1600 L, 130 fold greater than that of the reactor (12 L), a vacuum pump, and a steam generator supplying steam into the reactor.

### 2.4. Hydrothermal processes

The hydrothermal treatments were performed in pilot scale at fixed SP for 20 min. SMS (5 mm thickness) was placed in an aluminium rectangular container in reactor at a residual moisture content without any hydration step (Bahrani, 2012). Five SP levels were investigated: 1, 1.5, 2, 2.5 and 3 bar, corresponding to saturated steam temperatures of 100, 111, 120, 127 and 133 °C, respectively.

In DV-HMT, saturated steam was injected from atmospheric pressure up to processing SP level and maintained during 20 min. Processing time begins when SP reaches setting pressure. This step is followed by an abrupt decompression towards atmospheric pressure. While for RP-HMT and DIC reduced pressure of 50 mbar was established in the reactor before injection of live steam at fixed SP. After the maintaining phase, the abrupt decompression is performed towards atmospheric pressure for RP-HMT and vacuum pressure (50 mbar) for DIC. The presence of initial vacuum for both RP-HMT and DIC processes contributes to accelerate the transfer phenomenon associated with simultaneous heat and mass transfer by comparison with DV-HMT. At the beginning of hydrothermal treatment, the distribution of temperature field is non-homogenous, and it becomes homogenous throughout the material when equilibrium temperature is reached.

### 2.5. X-ray diffraction

Native and treated starch were equilibrated at 95% relative humidity (RH) using a saturated barium chloride solution, and the X-ray diffraction pattern was measured with Inel (France) X-ray equipment at 40 kV and 30 mA. The diagrams of diffraction were recorded according to the method of Debye-Scherrer in transmission. Cu K<sub>α1</sub>radiation ( $\lambda=0.154\text{ nm}$ ) was selected using a quartz monochromator. A curved position-sensitive detector CPS 120 was used to monitor diffracted intensities in the 0–120° 2θ range.

Diffractograms were all normalized at the same total scattering value, with  $2\theta$  ranging from 3 to  $30^\circ$ . The crystallinity ratio was calculated according to Wakelin method (Wakelin, Virgin, & Crystal, 1959) using spherulitic crystals and dry extruded potato starch as crystalline and amorphous standards respectively.

## 2.6. Polarised light microscopy

Dilute native and treated starches suspensions (1:20) were viewed under polarized light (magnifying 400 X) using a Leica microscope equipped with a CCD camera.

## 2.7. Differential scanning calorimetry (DSC)

DSC was conducted using a DSC Q100 (TA Instrument INC.) calibrated with indium. Starch samples (800 mg) were weighed into a stainless pan; distilled water was added to get a ratio of 1:9 (w/w) starch:water. Duplicated pans were hermetically sealed. The reference pan was filled with water. DSC runs were performed from 30 to  $110^\circ\text{C}$  at a heating rate of  $1.2^\circ\text{C}\cdot\text{min}^{-1}$ . The data were analyzed using Universal Analysis 2000 V4.4 software (TA Instrument-Waters LLC). Thermal transitions of starch samples are  $T_o$ : onset temperature;  $T_p$ : peak temperature;  $T_f$ : final temperature. The gelatinization temperature range (R) was calculated as  $(T_f - T_o)$ . The residual enthalpy ratio (RE) was calculated by:  $RE(\%) = \frac{\Delta H_G}{\Delta H_{\text{raw}}} \times 100$  where  $\Delta H_G$  is the enthalpy of gelatinization of residual structure of treated starch and  $\Delta H_{\text{raw}}$  that of native.

## 2.8. Determination of the amylose-lipid complex

We used the same equipment for measuring the thermal transition corresponding to the melting of amylose-lipid complexes: 90 mg of starch suspension (2:8 w/w starch:water) were sealed in a stainless pan and heated from 30 to  $140^\circ\text{C}$  with a heating rate of  $0.5^\circ\text{C}\cdot\text{min}^{-1}$ .  $\Delta H_M$  is the enthalpy of melting of the amylose-lipid complexes.

## 2.9. Particle size analysis

Granule size distribution was measured at room temperature using a Malvern Master Sizer (Malvern Instruments, Ltd) laser scattering analyser with a 300 mm Fourier cell (range 0.05–879  $\mu\text{m}$ ). Starch granules were diluted (1/10) with demineralized water at  $20^\circ\text{C}$  then dispersed into the sample dispersion unit (1 mL/100 mL water). The volume distribution was obtained according to the Mie scattering theory (Loisel, Maache-Rezzoug, & Esneault, 2006). From each distribution, the median volume diameter ( $D_{V,0.5}$ ) was calculated.

## 2.10. Statistical analysis

All analyses were determined in triplicate. The results were reported as the mean value and standard deviation with 95% confidence interval. The analysis of variance (ANOVA) was performed using *Statgraphics plus 5.1* software. Results were subjected to one-way analysis of variance (ANOVA) and *Fisher-test* to determine the significance of SP on the considered responses. The criterion for significance was  $P\text{-value} < 0.05$ .

**Table 1**

X-ray diffractometry characteristics of starch granules for samples hydrotreated by DV-HMT, RP-HMT and DIC at various processing pressures (1, 1.5, 2, 2.5 and 3 bar) during 20 min.

Sample	X-ray pattern	RC (%)
Native	A type	$25^{\pm 5\text{a}}$
DV-HMT		
1.0 bar	A type	30
1.5 bar	A type	25
2.0 bar	A type	25
2.5 bar	A + $V_h$	25
3.0 bar	$V_h$ type	nd
RP-HMT		
1.0 bar	A type	20
1.5 bar	A type	20
2.0 bar	A + $V_h$	nd
2.5 bar	$V_h$ type	nd
3.0 bar	$V_h$ type	nd
DIC		
1.0 bar	A type	25
1.5 bar	A type	20
2.0 bar	A + $V_h$	nd
2.5 bar	$V_h$ type	nd
3.0 bar	$V_h$ type	nd

nd; not determined, RC; Relative Crystallinity.

<sup>a</sup> The data represent the mean of three determinations.

## 3. Results and discussion

### 3.1. Structural characteristics

#### 3.1.1. X-ray diffraction and relative crystallinity

X-ray diffraction patterns of native and hydrothermal treated SMS with DV-HMT, RP-HMT and DIC at five SP levels (1, 1.5, 2, 2.5 et 3 bar) are given in Fig. 1. The values of relative crystallinity (RC) and the type of X-ray pattern are presented in Table 1. Native SMS exhibited typical A-type diffraction pattern (Imberty, Buléon, Tran, & Perez, 1991) with strong peaks at  $2\theta$  of about  $15^\circ$  and  $23^\circ$  and a doublet at  $17^\circ$  and  $18^\circ$ . This polymorphism type and RC value were fully preserved after treatment at  $100^\circ\text{C}$  (1 bar) and  $111^\circ\text{C}$  (1.5 bar), with a slight decrease in the peak intensities, primarily those focused at  $2\theta$  of  $15^\circ$ ,  $17^\circ$  and  $23^\circ$ . The reduction in RC became significant for RP-HMT and DIC treatments from  $120^\circ\text{C}$  (2 bar) and the A-type crystalline pattern was progressively reduced with increasing of SP ( $\geq 2$  bar). New peaks appeared at  $7.5^\circ$ ,  $13^\circ$  and  $19.5^\circ$  ( $20^\circ$ ), characteristics of a  $V_h$ -type crystalline pattern, revealing the formation of amylose-lipid complexes in SMS during treatments. The two crystalline types co-exist at intermediate conditions (2.5 and 2 bar with DV-HMT and RP-HMT/DIC respectively) while the typical peaks of A-type X-ray diffraction pattern were almost replaced by  $V_h$ -type for more severe conditions (3 and 2.5 bar for DV-HMT and RP-HMT/DIC, respectively). The resolution and intensity of the new peaks attest that amylose-lipid complexes can reorganize in a crystalline packing as a result of hydrothermal treatments. In these conditions, RC values could not be determined due to the lack of standard crystalline  $V_h$ -type. According to Le Bail et al. (1999), despite its small concentration, the lipid phase present mainly in cereals starches has a large influence on starch properties, particularly in complexing amylose.

Moisture content promotes the effects of HMT on starch crystallites structure disruptions causing the breaking of hydrogen bonds. Wang et al. (2016) showed for SMS that the intensity and nature of phase transitions induced in crystalline structure are related to temperature and moisture content. The higher moisture levels caused a reduction in the peak visibility, indicating that disorganization events occurred in the amorphous-crystalline lamellae

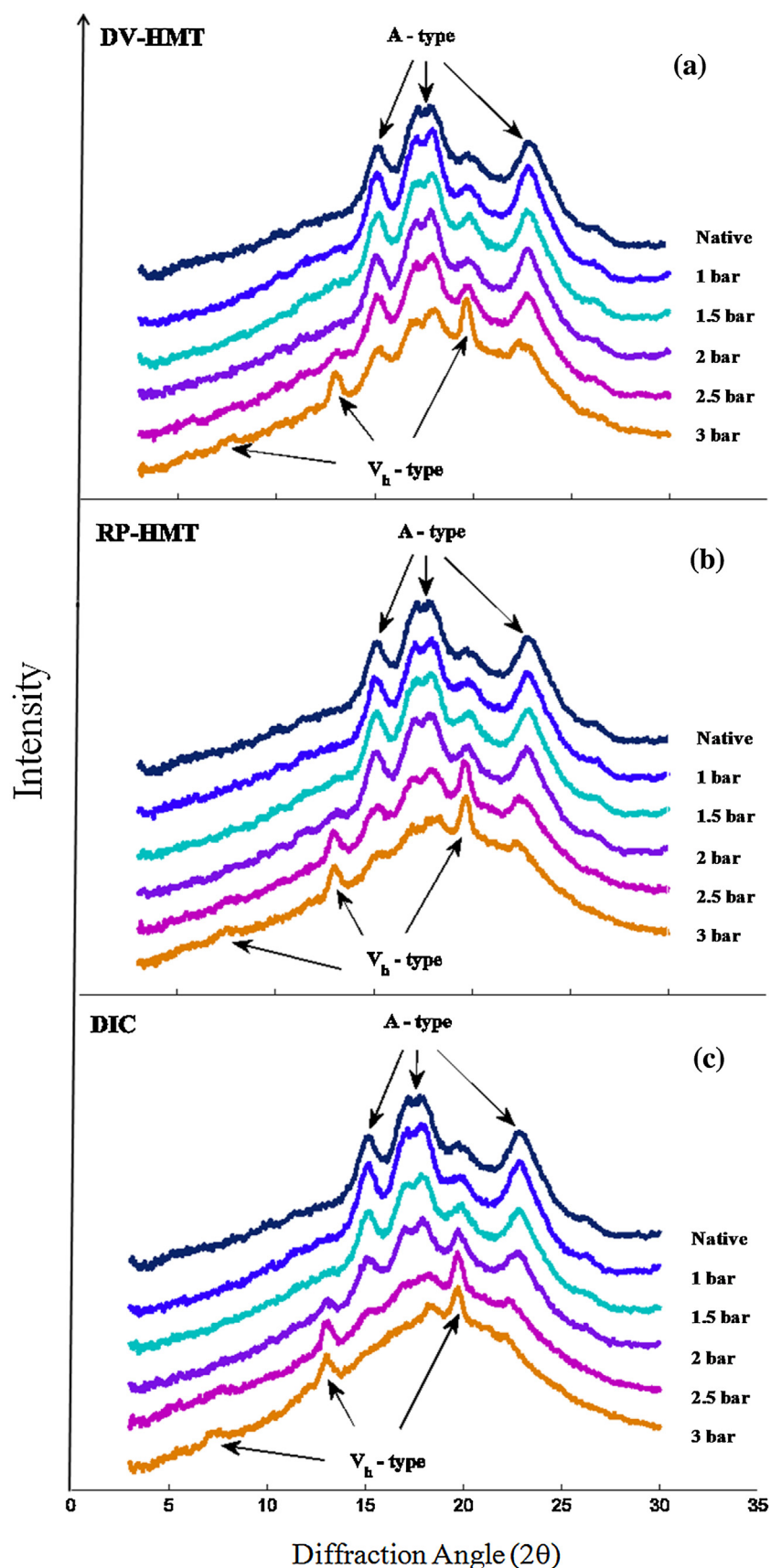


**Fig. 1.** X-ray diffraction patterns of native SMS and treated with DV-HMT (a), RP-HMT (b) and DIC (c) at various SP during 20 min.

during HMT by Sui et al. (2015) observed that the RC decreased to a greater extent with increasing moisture content.

### 3.1.2. Polarized light microscopy

Starch granules exhibited a typical birefringence cross under polarized light, since the ordered microscopic observations under polarized light of native and SMS treated with DV-HMT (A), RP-HMT (B) and DIC (C) are presented in Fig. 2. Native and treated starch granules at low conditions (SP = 1 bar) exhibited a typical birefringence cross under polarized light (Fig. 2A<sub>1</sub>, B<sub>1</sub> and C<sub>1</sub>), confirming the preservation of crystallinity. Birefringence also reflects the average radial orientation of helical structures (Vermeylen et al., 2006), which is independent from crystallinity. The conservation of this organization into the granules is indicative of low internal changes compared to the native. Birefringence predominantly kept unchanged in DV-HMT and RP-HMT starch treated at SP of 1.5 bar (Fig. 2A<sub>2</sub> and B<sub>2</sub>). In contrast, for the same conditions, granules starch treated by DIC (Fig. 2C<sub>2</sub>) displayed a reduced birefringence brightness at the periphery, with enlarged dark area at the centre. Vermeylen et al. (2006) showed on HMT potato starch, that the formation of voids at the granule centre grows with the temperature. However, from SP of 2 bar RP-HMT and DIC starch resulted in total disappearance of birefringence (Fig. 2B<sub>3</sub>-B<sub>4</sub> and C<sub>3</sub>-C<sub>4</sub>) whereas in DV-HMT (Fig. 2A<sub>3</sub>-A<sub>4</sub>), the birefringence slightly decreased but the cross polarization remained visible in some granules. These results confirmed the almost total melting of A-type crystalline structure of granules observed by X-ray diffraction.

## 3.2. Thermal properties

### 3.2.1. Gelatinization

Gelatinization parameters of native and treated starch are summarized in Table 2 and DSC curves describing the thermal behaviour of starch are presented in Fig. 3. For each treatment, the peak of gelatinization appeared in a single endotherm between 55 and 85 °C, except for starch treated by DIC process (Fig. 3c), where no transition was observed at SP of 3 bar, indicating that the residual structure of starch has completely melted during the treatment. The gelatinization temperatures (T<sub>o</sub>, T<sub>p</sub>, T<sub>f</sub>) of native starch were 56.4 °C, 66.9 °C and 78.1 °C, respectively. These values have systematically increased after treatment compared to the native, suggesting that the rearrangements of starch molecular chains took place during treatments to form a specific molecular order (helices and/or crystallites) with an improved thermal stability. This is clearly visible by the systematic shift of gelatinization endotherms to larger transition temperatures. The shift was more pronounced at higher SP and the intensity of changes induced by the different processes was displayed following this order: DIC > RP-HMT > DV-HMT. Increasing of transition temperatures after HMT has been attributed to structural changes within starch granules, which involve amylose–amylose and amylose–lipid interactions (Hoover & Vasanthan, 1994), that reduce the mobility in amorphous regions. This reduction, as a result of HMT, requires a higher temperature to cause swelling and disruption of crystalline regions. For all processes, the enthalpy of gelatinization ( $\Delta H_G$ ) gradually decreased as the SP increased (Table 2).  $\Delta H_G$  of 12.2 J/g (native) decreased from 11.9 up to 4.1 J/g, from 11.3 up to 2 J/g and from 10.9 up to 0 J/g for SMS treated by DV-HMT, RP-HMT and DIC at 1 and 3 bar, respectively. Enthalpy reduction after hydrothermal treatment reflects partial melting of some starch granules whose crystalline structure is less stable (Arns et al., 2015; Maache-Rezzoug et al., 2011). In more intense conditions (DIC at SP of 3 bar/133 °C), the absence of endothermic transition may suggest that the energy released was sufficient to completely melt the crystalline structure. The same trend is observed with the residual enthalpy ratio (RE), which decreased when SP increased (Table 2). RE reached 33.9%, 16.4% and 0% at 3 bar

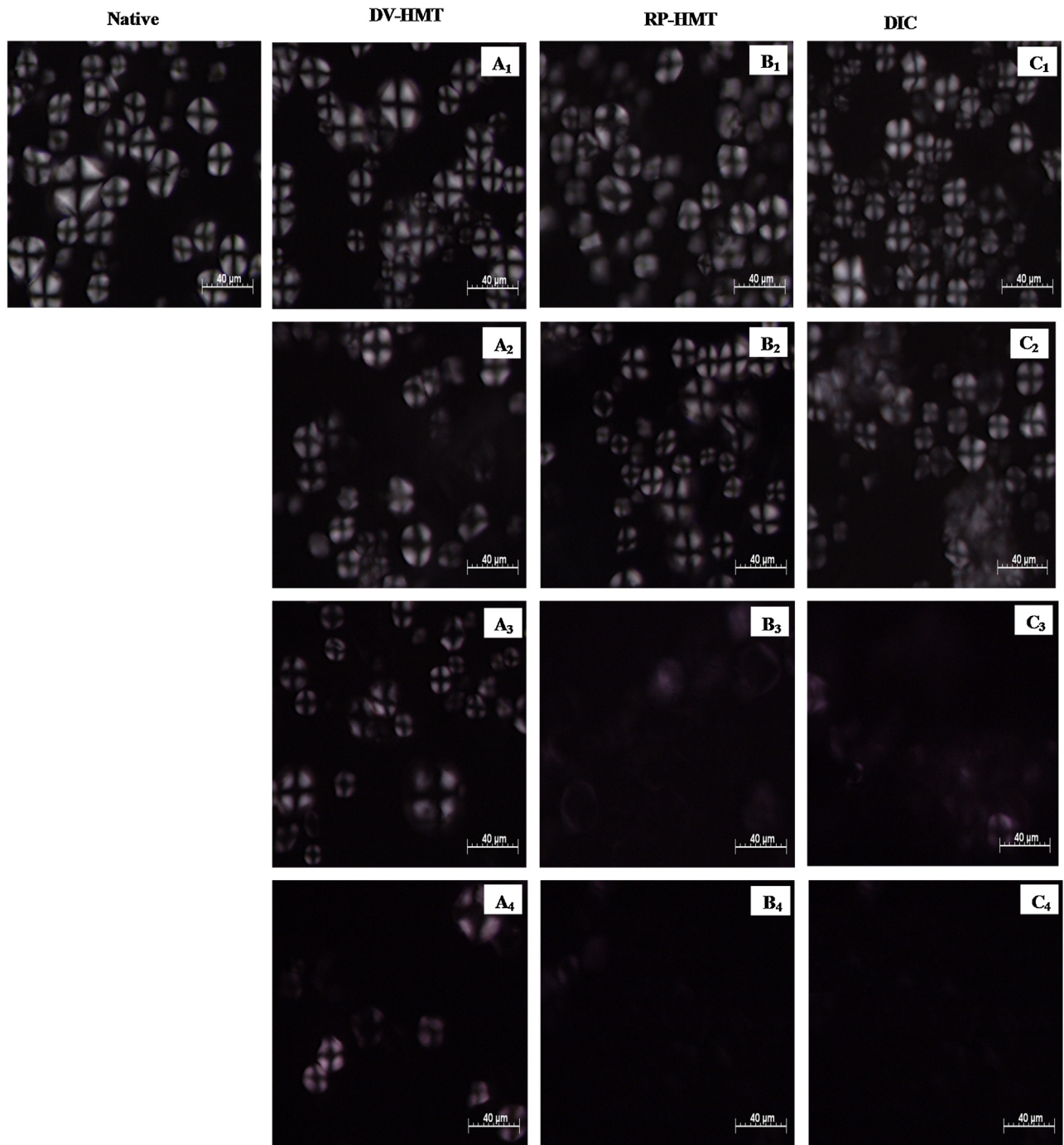
with DV-HMT, RP-HMT and DIC, respectively. As for gelatinization temperatures, the intensity of structural changes is influenced not only by steam pressure level, therefore by the temperature and moisture content, but also by the mechanical effect produced during the abrupt decompression towards vacuum. During HMT by direct streaming, the absorption of latent heat of steam condensation caused an increase in the moisture content of starch as the SP and processing time increased (Zarguili et al., 2009). The difference in physicochemical changes produced by the three treatments is mainly due to the difference in moisture content between DV-HMT and RP-HMT/DIC. At SP of 2 bar (120 °C), the moisture content was 20% for DV-HMT and 24% for RP-HMT/DIC. As the water content was the same for RP-HMT and DIC, the difference between them is linked to the more intense mechanical effect induced by DIC process. The strong effect of the moisture content (in the range of 18 to 20%) on enthalpy reduction has already been shown by Adebowale and Lawal (2003) and Vermeylen et al. (2006) for which the highest temperatures and moisture contents of treated potato starch provoked the largest changes on gelatinization enthalpy.

Fig. 4 presents the relationship between processing pressure and thermal properties of treated starch during the process of gelatinization. The gelatinization temperatures (T<sub>o</sub>, T<sub>p</sub>, T<sub>f</sub>) of treated starch increased with pressure (Fig. 4a–c). The highest differences in temperature between native and treated starch were observed for T<sub>o</sub> (Fig. 4a). The differences were of 7.3, 9.1 and 12.1 °C for DV-HMT, RP-HMT and DIC, respectively. This proves the greater sensitivity of T<sub>o</sub> to show changes in the internal structure of starch granules. According to Chung, Hoover and Liu (2009) T<sub>o</sub> represents the melting of the weaker crystallites, those involving low energy to melt. Thus the HMT treatments contributed to improve the thermal stability of crystallites as suggested by Ji, Ao, Han, Jane and BeMiller (2004) who report that T<sub>o</sub> could be an indicator of the degree of crystallites perfection of starch granules.

For the three treatments at low SP (1 bar), the gelatinization temperature range (R) remained similar to that of the native and the narrowing became significant from 1.5 bar (Fig. 4d). Beyond SP of 2 bar, a significant decrease of R was observed for starch treated by DIC process compared to the two other. R decreased from 21.7 °C (native) to 19.9 °C (DV-HMT), 19.4 °C (RP-HMT) and 15.3 °C (DIC). The mechanical effect produced by the abrupt decompression towards the vacuum, more intense for DIC process contributed to disrupt the organized crystalline structure of starch granules, while its effect is reduced in RP-HMT since the decompression is carried out to atmospheric pressure. The narrowing of temperature range of treated starches have already observed by Maache-Rezzoug et al. (2011), who attributed it to increasing of the degree of homogeneity of crystallites within the granules. According to Fredriksson, Silverio, Andersson, Eliasson and Aman (1998), an extended temperature range reflected a wide range of crystals stability. Consequently the heterogeneity of crystallites broadened the gelatinization temperature range. Our results suggest that the three treatments have induced first the melting of crystallites from low stability, those requiring less energy and a reinforcement of the interactions between the remaining crystallites chains. Accordingly, the residual structure after treatment contained homogeneous crystallites with a greater stability.

### 3.2.2. Amylose–lipid complex formation

Differential scanning calorimetry (DSC) was used to study the thermal properties of amylose–lipid complexes formed during HMT treatment of starch by the three processes identified by X-ray diffraction analysis (3.1.1 Section). Fig. 5 displays the thermograms recorded on native and DIC treated starch at different conditions and analysis of those treated by DV-HMT and RP-HMT processes (not shown) are given in Table 2.



**Fig. 2.** Microscopic observations in polarized light of native and treated maize starch with DV-HMT (A), RP-HMT (B) and DIC (C) processes at 1 bar (1), 1.5 bar (2), 2 bar (3) and 3 bar (4) during 20 min.

The first endotherm corresponds to the gelatinization process of crystalline lamellae of the intact structure of native and the residual structure of the treated starch as previously discussed (Section 3.2.1). The gelatinization phenomenon, widely studied by DSC, is observed as an endothermic transition, which basically reflects an order-disorder transition resulting from the melting of the crystalline regions in the starch granule (Donovan, 1979). Exothermic transition peak ①, observed on native and treated granules for lowest processing conditions (1 and 1.5 bar), is relative to the extra-granular crystallization of amylose and lipid during DSC heating. These inclusion complexes are known to be formed during gelatinization with endogenous or added lipids (Morrison,

Tester, Snape, Law & Gidley, 1993). The formation of these complexes was followed by an endothermic transition ② at about 95 °C, corresponding to their melting. Amylose-lipid complexes rarely exist in native cereal starches but are usually formed upon heating. The complex formation ability, i.e. the amount of complex formed under certain conditions, is related to the phase behaviour of the complexing agent (Larsson, 1980) and the structure of complex formed depends on the temperature at which complexation occurred (Gelders, Vanderstukken, Goesaert & Delcour, 2004) as well as the temperature rate. Beyond 1.5 bar, the transitions ① and ② were reduced since amylose-lipid complexes have already been formed inside the starch granules during treatment. As evidenced

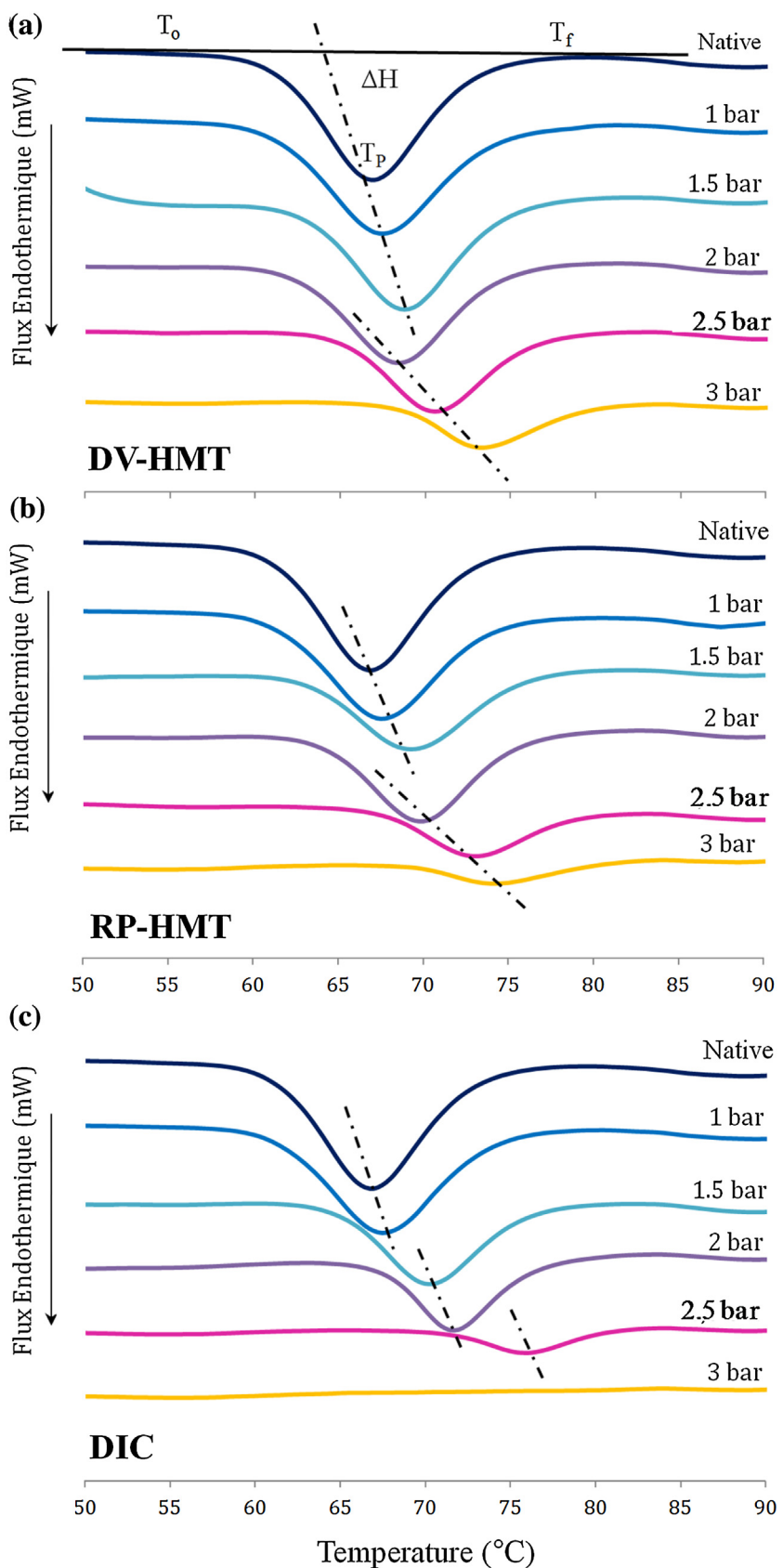


**Fig. 3.** Differential Scanning Calorimetry patterns of native and treated SMS by DV-HMT (a), RP-HMT (b) and DIC (c) at different SP and 20 min. Heating rate:  $1.2^{\circ}\text{C}.\text{min}^{-1}$ .

**Table 2**

Thermal properties of native and treated SMS by DV-HMT®, RP-HMT® and DIC® at five steam pressure (1, 1.5, 2, 2.5 and 3 bar) for 20.

Sample	Gelatinization						Amylose-lipid complex		
	$T_0$ (°C)	$T$ (°C)	$T_f$ (°C)	R(°C)	$\Delta H$ (J/g)	RE (%)	$T^*$ (°C)*	$T$ (°C)*	$\Delta H$ (J/g)
Native DV-HMT	56.4 $\pm$ 0.37	66.9 $\pm$ 0.10	78.1 $\pm$ 0.12	21.7	12.2 $\pm$ 0.3	100	–	–	–
1.0 bar	57.1 $\pm$ 0.45	67.2 $\pm$ 0.38	79.1 $\pm$ 0.08	22	11.9	97.4	–	–	–
1.5 bar	59.6 $\pm$ 0.71	68.8 $\pm$ 0.41	80.0 $\pm$ 0.24	20.4	10.5	86.3	106.0 $\pm$ 0.81	112.5 $\pm$ 0.7	0.51 $\pm$ 0.01
2.0 bar	58.70 $\pm$ 0.53	68.4 $\pm$ 0.19	79.5 $\pm$ 0.19	20.8	9.6	78.3	104.7 $\pm$ 0.91	112.3 $\pm$ 0.3	0.97 $\pm$ 0.09
2.5 bar	61.3 $\pm$ 0.39	70.4 $\pm$ 0.26	81.2 $\pm$ 0.21	19.9	7.7	62.8	100.5 $\pm$ 0.78	112.0 $\pm$ 0.6	1.54 $\pm$ 0.13
3.0 bar	63.7 $\pm$ 0.27	73.2 $\pm$ 0.38	83.3 $\pm$ 0.14	19.6	4.1	33.9	101.8 $\pm$ 0.56	113.2 $\pm$ 0.4	2.30 $\pm$ 0.23
RP-HMT	–	–	–	–	–	–	–	–	–
1.0 bar	56.9 $\pm$ 0.29	67.4 $\pm$ 0.41	78.8 $\pm$ 0.27	21.8	11.3	92.5	–	–	–
1.5 bar	60.1 $\pm$ 0.337	69.3 $\pm$ 0.36	80.1 $\pm$ 0.19	20	8	65.5	104.7 $\pm$ 0.77	112.8 $\pm$ 0.9	0.55 $\pm$ 0.07
2.0 bar	61.7 $\pm$ 0.41	70.0 $\pm$ 0.27	80.4 $\pm$ 0.31	18.7	7.9	64.5	105.0 $\pm$ 0.66	112.3 $\pm$ 1.2	1.01 $\pm$ 0.10
2.5 bar	63.9 $\pm$ 0.53	73.0 $\pm$ 0.24	83.4 $\pm$ 0.15	19.4	4.4	36.1	100.5 $\pm$ 0.49	112.8 $\pm$ 0.7	2.39 $\pm$ 0.42
3.0 bar	65.5 $\pm$ 0.32	74.2 $\pm$ 0.17	83.9 $\pm$ 0.21	18.4	2	16.4	102.3 $\pm$ 0.53	114.4 $\pm$ 1.0	2.67 $\pm$ 0.37
DIC	–	–	–	–	–	–	–	–	–
1.0 bar	56.6 $\pm$ 0.12	67.5 $\pm$ 0.38	78.6 $\pm$ 0.31	22	10.9	89	–	–	–
1.5 bar	60.6 $\pm$ 0.27	70.0 $\pm$ 0.23	80.7 $\pm$ 0.18	20	7.6	62.4	106.2 $\pm$ 0.77	112.7 $\pm$ 0.6	0.62 $\pm$ 0.10
2.0 bar	63.7 $\pm$ 0.39	71.7 $\pm$ 0.31	82.1 $\pm$ 0.25	18.4	5.6	46.2	104.0 $\pm$ 0.86	112.6 $\pm$ 0.9	1.15 $\pm$ 0.08
2.5 bar	68.5 $\pm$ 0.25	76.0 $\pm$ 0.26	83.8 $\pm$ 0.26	15.3	1.8	14.4	100.5 $\pm$ 0.93	112.8 $\pm$ 1.1	2.49 $\pm$ 0.17
3.0 bar	–	–	–	–	0	0	101.2 $\pm$ 0.57	116.1 $\pm$ 0.8	2.74 $\pm$ 0.29

$T_0$ : onset temperature;  $T_p$ : peak temperature;  $T_f$ : final temperature; R: temperature range, calculated as  $(T_f - T_0)$ . Values are means of triplicate determinations  $\pm$  standard deviation.  $\Delta H_G$ : enthalpy of gelatinization. RE (%): residual enthalpy ratio.  $T_0^*$ : onset melting temperature;  $T_p^*$ : peak melting temperature.  $\Delta H_M$ : enthalpy of melting of the V<sub>h</sub>-amylose-lipid complex.

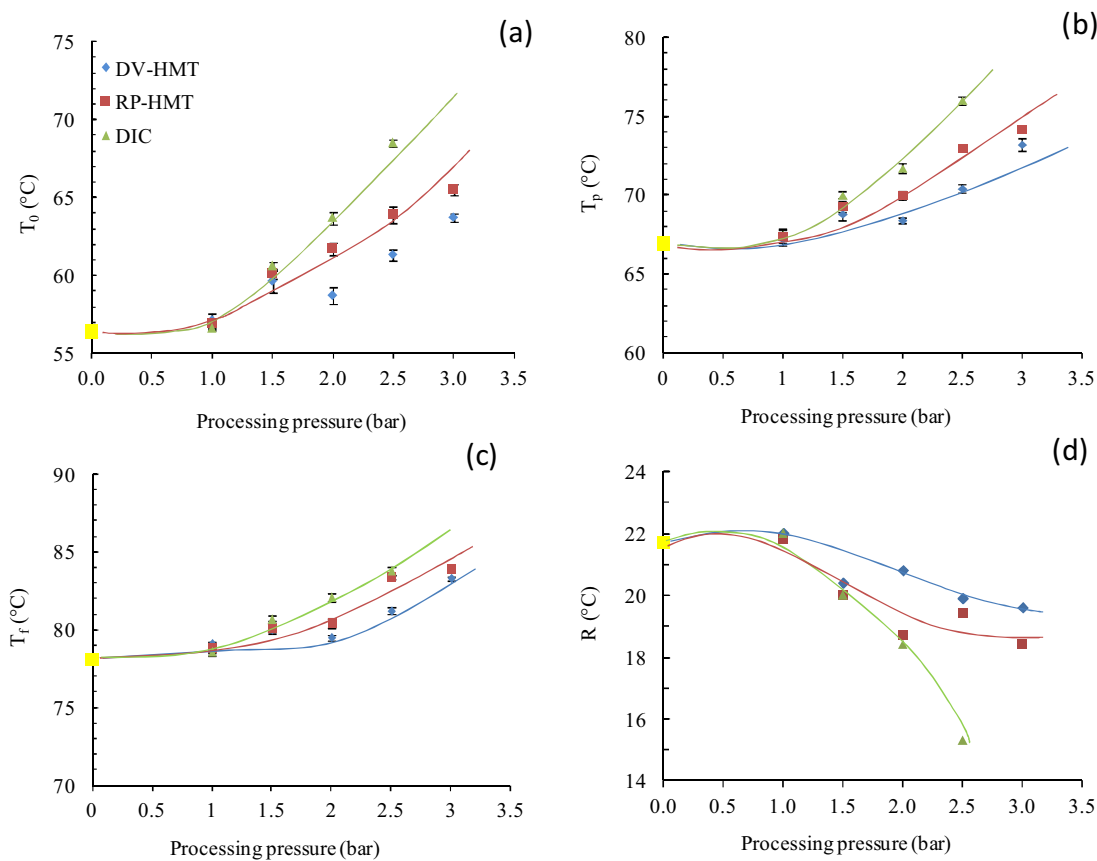


**Fig. 4.** Relationship between processing pressure and gelatinization temperatures of SMS treated by DV-HMT, RP-HMT and DIC.

by the emergence of the endothermic transition peak ③, apparent at higher temperatures, corresponding to the melting or dissociation of V<sub>h</sub>-amylose structure formed during DIC process. At 3 bar a single melting peak remained visible on the thermogram suggesting a large intra-granular crystallization of amylose and lipid. The amylose-lipid complexes formed during DV-HMT, RP-HMT and

DIC exhibited a thermal transition at about 115 °C (Table 2) and the enthalpies of the melting of these complexes ( $\Delta H_m$ ) increased significantly from 2 bar  $\Delta H_m$  reflects the relative amount of formed complexes in the granules (Tufvesson, Wahlgren, & Eliasson, 2003), these values varied from 1.54 to 2.30 J/g for DV-HMT, from 2.39 to 2.67 J/g for RP-HMT and from 2.49 to 2.74 J/g for DIC, at 2.5 and

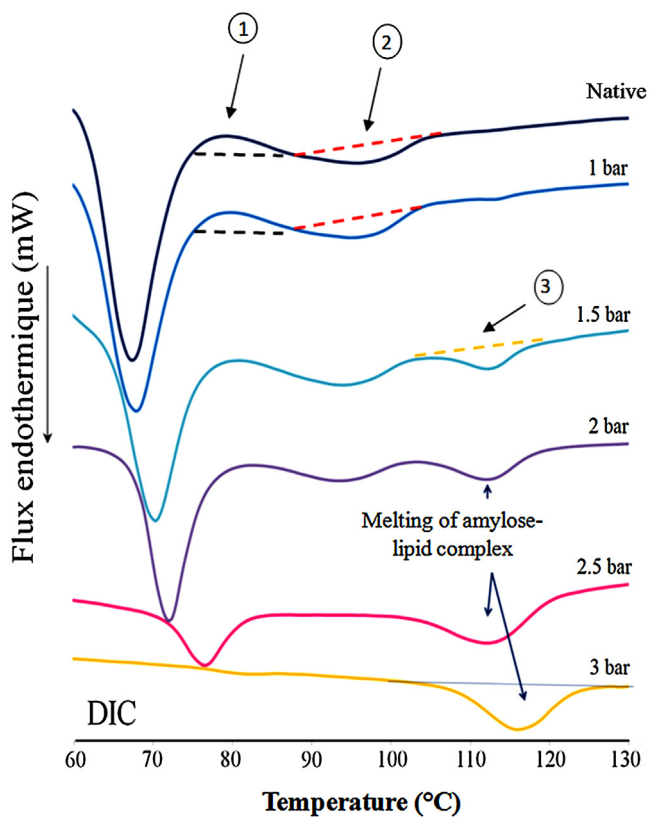


**Fig. 5.** Phase transition peaks of native and SMS treated with DIC process. ① : Exothermic formation of amylose-lipid complexes during DSC heating. and ③ : Endothermic transition peaks corresponding to the melting of amylose-lipid complex formed during DSC and DIC treatment, respectively. Heating rate:  $0.5\text{ }^{\circ}\text{C}.\text{min}^{-1}$ .

3 bar, respectively. Also, for the same conditions the endothermic peaks were shifted to higher melting temperatures. At SP of 3 bar,  $T_p$  were  $113.2\text{ }^{\circ}\text{C}$ ,  $114.4\text{ }^{\circ}\text{C}$  and  $116.1\text{ }^{\circ}\text{C}$  for DV-HMT, RP-HMT and DIC treatment, respectively.

Amylose-lipid complex formation is affected by several factors: the more important are the process temperature and moisture content. Le Bail et al. (1999) observed a  $V_h$ -type diffraction pattern around  $110\text{--}115\text{ }^{\circ}\text{C}$ , after heating of SMS in excess of water (65% moisture content). The authors suggested that the important leaching of amylose enables the extra-granular crystallization of amylose and lipid. In contrast, at low moisture contents, the treatment enhanced the formation of the amylose-lipid complexes inside the swollen granules due to the reduction of amylose solubilization. Therefore, in our study, the three HMT treatments caused the formation of amylose-lipid complexes inside the starch granules, due to the low moisture content (<30%) prevailing. According to Buléon, Colonna, Planchet and Ball (1998) the amylose chains are involved either in isolated inclusion complexes or in crystalline packing arrangements. Only this later structure can be detected by X-ray diffraction analysis in the form of  $V_h$ -type diffraction diagram.

### 3.3. Granule morphology

#### 3.3.1. Analysis of aggregates formation

A progressive increase of median diameter in volume ( $D_{v,0.5}$ ) of granules was observed after each hydrothermal treatment (Table 3). The details of the size distributions of native and treated SMS with the three processes were previously given by Bahrani et al. (2012).  $D_{v,0.5}$  of  $13.73\text{ }\mu\text{m}$  for native starch increased from  $15.50$  to  $21.70\text{ }\mu\text{m}$  for DV-HMT at 1 and 2.5 bar, from  $15.90$  to

**Table 3**

Analysis of size distribution of starch granules for samples hydrotreated with DV-HMT, RP-HMT and DIC at various steam pressures (1, 1.5, 2, 2.5 and 3 bar) during 20 min.

Sample	$D_{v,0.5} (\mu\text{m})$	LC (%)	ACN
Native	$13.73 \pm 1.10$	0	–
DV-HMT			
1.0 bar	$15.50 \pm 0.07$	2.6	0
1.5 bar	$16.47 \pm 0.06$	13.7	0
2.0 bar	$16.88 \pm 0.12$	21.7	0
2.5 bar	$21.70 \pm 0.16$	37.2	1
3.0 bar	$36.20 \pm 0.45$	66.1	2
RP-HMT			
1.0 bar	$15.90 \pm 0.14$	7.5	0
1.5 bar	$17.30 \pm 0.07$	34.5	0
2.0 bar	$17.77 \pm 0.49$	35.5	0
2.5 bar	$33.74 \pm 0.53$	63.9	2
3.0 bar	$60.63 \pm 0.15$	83.6	3
DIC			
1.0 bar	$16.37 \pm 0.10$	11	0
1.5 bar	$19.90 \pm 0.30$	37.6	0
2.0 bar	$22.70 \pm 0.60$	53.8	1
2.5 bar	$56.38 \pm 0.84$	85.6	3
3.0 bar	$138.30 \pm 3.80$	100	5

All data represent the mean of three determinations.

$D_{v,0.5}$ ; median volume diameter, LC; Loss of Crystalline structure, ACN; Aggregates Class Number.

$17.77\text{ }\mu\text{m}$  and from  $16.37$  to  $22.70\text{ }\mu\text{m}$  for RP-HMT and DIC at 1 and 2 bar, respectively. At severe processing conditions, SP of 3 bar for DV-HMT and from 2.5 bar for RP-HMT and DIC, the values of  $D_{v,0.5}$  clearly confirmed the presence of aggregates.

The mechanism of aggregates formation was investigated by Herrera-Goímez, Canoíñico-Franco and Ramos (2005) on maize starch granules cooked at reduced moisture content for various temperatures. The authors showed that these limited conditions induced formation of aggregates of different sizes that are held together by gelatinized granules showing no cross-polarization. As shown in Section 3.2.1, increasing of saturated steam pressure had as a consequence the partial or total melting of starch granules. Thus contributing to the formation of aggregates for which the number of melted granules has a direct effect on their size. Fig. 6A presents the variation of  $D_{v,0.5}$  as a function of the loss of crystalline structure (LC), estimated by the relationship:  $LC(\%) = (100 - RE)$ . The results clearly showed that the particle size distribution depends on the melting extent of crystalline structure.  $D_{v,0.5}$  values correspond to the size of individual particles ( $LC < 40\%$ ), achieved with low to moderate treatment ( $SP \leq 2\text{ bar}$ ). As the fraction of melted granules was low thus the number of particles glued together was limited. For  $LC > 40\%$ ,  $D_{v,0.5}$  values reflected a typical size of aggregates. Indeed, beyond SP of 2 bar the melted fraction increased and more complex aggregates have been formed, especially for starch treated with DIC at 3 bar, for which a total melting of crystalline structure occurred. These results were confirmed by scanning electron microscopy analysis (Bahrani et al., 2012) for SMS treated under moderate conditions which showed individual granules with a regular spherical shape like native granules, or irregular forms, mainly with DIC treated starch. According to Herrera-Goímez, Canoíñico-Franco and Ramos (2002) the spherical shape suggests that the granule is not gelatinized while an irregular shape indicates that the granule has been gelatinized, at least partially.

#### 3.3.2. Analysis of aggregates size

In order to link the impact of investigated processes to the size of aggregates we plotted in Fig. 6B the variation of  $D_{v,0.5}$  as a function of the Aggregate Class Number (ACN). Herrera-Goímez et al. (2005) defined 5 ACN according to the cooking degree of maize starch. Class 0 corresponds to the size of individual particles such as

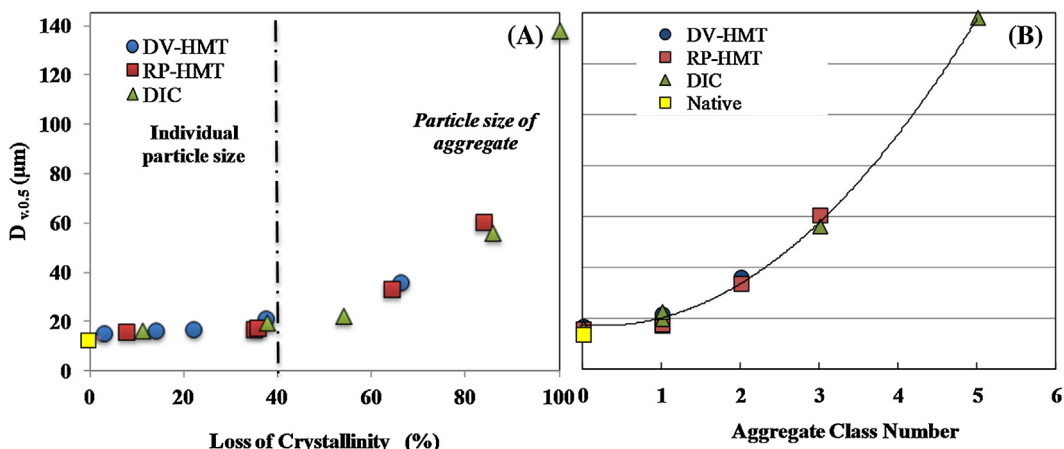


**Fig. 6.** Influence of the loss of crystallinity on the median volume diameter ( $D_{v,0.5}$ ) of native and treated SMS by the three processes (A) at different SP values. The representative  $D_{v,0.5}$  for each aggregate class number (B).

the native. Class 1 coincides with the presence of some gelatinized granules surrounded by a limited number of particles partially or non-gelatinized. Class 2 is composed of aggregates of size larger than the precedent Class, formed by aggregates of Class 1 glued together. The authors observed that completely gelatinised granules formed the Class 4.

Using the typical relation of power law model proposed by the same authors ( $T \approx 15.8 \times 1.6^n$ ), for each size of aggregates ( $T$ ) the class number ( $n$ ) was determined (Table 3).  $15.8 \mu\text{m}$  corresponds to an average value of individual particles size. Fig. 6B showed that the  $D_{v,0.5}$  values of treated granules under different conditions reflect the size distribution of aggregates particle. For DV-HMT and RP-HMT at SP ranging from 1 to 2 bar and for DIC at 1 and 1.5 bar, the partially melted granules, did not permit the formation of aggregates and therefore the size of individual particles correspond to that of Class 0. The progress of melting phenomenon with the intensification of processing conditions (DV-HMT and DIC at 2.5 and 2 bar, respectively) contributed to the appearance of small aggregates forming Class 1, resulting from the presence of a few fully melted granules surrounded by a limited number of partially melted or intact granules. Starch granules treated with DV-HMT at 3 bar and RP-HMT at 2.5 bar formed aggregates of larger sizes corresponding to Class 2. The extent of the loss of crystallinity (DIC and RP-HMT at 2.5 and 3 bar, respectively) has contributed to increasing in aggregates size, thus forming Class 3. As DIC treatment at 3 bar resulted in the complete melting of starch structure ( $LC = 100\%$ ), the formed aggregates have the larger sizes, with  $D_{v,0.5} = 138 \mu\text{m}$ , representing Class 5. The particles glued together by melted granules were favoured by the direct contact between steam and starch granules during treatments and by the mechanical impact during the release of pressure. From the results, a shifting of one Class was observed between the three processes; at  $SP = 2.5$  bar,  $n$  was of 1, 2 and 3, confirming thus the intermediate position of RP-HMT treatment.

#### 4. Conclusion

The physicochemical and structural properties of SMS depended on the type of process and steaming conditions. The intensity of modifications followed this order: DIC > RP-HMT > DV-HMT. The extent of the physicochemical changes is due to the presence of initial vacuum for RP-HMT and DIC processes, contributing to the intensification of heat and mass transfers compared to DV-HMT in which this step is not present. Moreover, at the end of DIC process, the mechanical action induced by the sudden decom-

pression towards vacuum contributed to alter crystalline structure and weaken the starch granules. The results showed that the general effects on starch granules were the decrease of the relative crystallinity, the decrease of the enthalpy and the temperature range of gelatinization as well as an increase in the gelatinization temperatures. Therefore, the hydrothermal treatments contributed to increase the thermal stability of starch granules by promoting the strengthening of the ties which making the structure more cohesive. From 2 bar, the decrease in relative crystallinity was accompanied by the change from A-type crystalline structure to V<sub>h</sub>-type, revealing the formation of amylose-lipid complexes during the steaming. The treatments modified the shape and size distribution of starch granules. The increasing of size was due both to the improvement of swelling capacity of granules but also, for the intense conditions, to the formation of aggregates of various sizes, favoured by the direct contact of particles and steam. The number of melted granules had a direct impact on the aggregate sizes. For a processing pressure lower than 2 bar, the melted fraction of granules was low, therefore the glued particles was limited, leading to the formation of small-diameter aggregates. Beyond 2 bar, the melting phenomenon of starch granules progressed and aggregates of large size appeared mainly for starch treated by DIC at 3 bar for which a total fusion of granules occurred.

#### Acknowledgement

We express our acknowledgment to Bruno Pontoire for his special support in the realisation of X-ray diffraction analysis.

#### References

- A.O.A.C. (1999). *Association of Official Analytical Chemists*.
- Adebawale, K. O., & Lawal, O. S. (2003). Microstructure: Physicochemical properties and retrogradation behaviour of Mucuna bean (*Mucuna pruriens*) starch on heat moisture treatments. *Food Hydrocolloids*, 17, 265–272.
- Arns, B., Bartz, J., Radunz, M., Evangelho, J. A. D., Pinto, V. Z., Zavarce, E. D. R., et al. (2015). Impact of heat-moisture treatment on rice starch: Applied directly in grain paddy rice or in isolated starch. *LWT-Food Science and Technology*, 60, 708–713.
- Bahrani, S.-A., Loisel, C., Doublier, J.-L., Rezzoug, S.-A., & Maache-Rezzoug, Z. (2012). Role of vacuum steps added before and after steaming treatment of maize starch. *Impact on Pasting, Morphological and Rheological Properties*. *Carbohydrate Polymers*, 89, 810–820.
- Bahrani, S.-A., Loisel, C., Maache-Rezzoug, Z., Della Valle, D., & Rezzoug, S.-A. (2013). Rheological and viscoelastic properties of corn starch suspension modified by hydrothermal process: Impacts of process intensification. *Chemical Engineering and Processing: Process Intensification*, 64, 10–16.
- Bahrani, S.-A., Monteau, J.-Y., Rezzoug, S.-A., Loisel, C., & Maache-Rezzoug, Z. (2014). Physics-based modeling of simultaneous heat and mass transfer

- intensification during vacuum steaming processes of starchy material. *Chemical Engineering and Processing: Process Intensification*, 85, 216–226.
- Bahrani, S.-A. (2012). *Physico-chemical modifications of starch by hydrothermal processes: contribution to the investigation of simultaneous heat and mass transfer*. Ph.D. dissertation, University of La Rochelle.
- Biliaderis, C. G., Page, C. M., Maurice, T. J., & Juliano, B. O. (1986). Thermal characterization of rice starch: A polymeric approach to phase transitions of granular starch. *Journal of Agricultural and Food Chemistry*, 34, 6–14.
- Buléon, A., Colonna, P., Planchot, V., & Ball, S. (1998). Starch granules: Structure and biosynthesis. *International Journal of Biological Macromolecules*, 23, 58–112.
- Chung, H.-J., Hoover, R., & Liu, Q. (2009). The impact of single and dual hydrothermal modifications on the molecular structure and physicochemical properties of normal maize starch. *International Journal of Biological Macromolecules*, 44, 203–210.
- Chung, H. J., Liu, Q., & Hoover, R. (2009). Impact of annealing and heat-moisture treatment on rapidly digestible, slowly digestible and resistant starch levels in native and gelatinized corn, pea and lentil starches. *Carbohydrate Polymers*, 75, 436–447.
- Collado, L. S., & Corke, H. (1999). Heat-moisture treatment effects on sweet potato starches differing in amylose content. *Food Chemistry*, 65, 329–346.
- Donovan, J. W. (1979). Phase transitions of the starch-water system. *Biopolymers*, 18, 263–275.
- Fredriksson, H., Silverio, J., Andersson, R., Eliasson, A. C., & Aman, P. (1998). The influence of amylose and amylopectin characteristics on gelatinization and retrogradation properties of different starches. *Carbohydrate Polymers*, 35, 119–134.
- Gelders, G. G., Vanderstukken, T. C., Goesaert, H., & Delcour, J. A. (2004). Amylose-lipid complexation: A new fractionation method. *Carbohydrate Polymers*, 56, 447–458.
- Gunaratne, A., & Hoover, R. (2002). Effect of heat treatment on the structure and physicochemical properties of tuber and root starches. *Carbohydrate Polymers*, 49, 425–437.
- Herrera-Goímez, A., Canoíñico-Franco, M., & Ramos, G. (2002). Aggregation in cooked maize starch. *Carbohydrate Polymers*, 50, 387–392.
- Herrera-Goímez, A., Canoíñico-Franco, M., & Ramos, G. (2005). Aggregate formation and segregation of maize starch granules cooked at reduced moisture conditions. *Starch/Stärke*, 57, 301–309.
- Hoover, R., & Manuel, H. (1996). The effect of heat-moisture treatment on the structure and physicochemical properties of normal maize, waxy maize, dull waxy maize and amyloamaize starches. *Journal of Cereal Science*, 23, 153–162.
- Hoover, R., & Vasanthan, T. (1994). Effect of Heat-Moisture Treatment on the structure and physicochemical properties of cereal, tuber, and legume starches. *Carbohydrate Research*, 252, 33–53.
- Huang, Z.-Q., Lu, J.-P., Li, X.-H., & Tong, Z.-F. (2007). Effect of mechanical activation on physico-chemical properties and structure of cassava starch. *Carbohydrate Polymers*, 68, 128–135.
- Hublin, L. (1994). *Influence des caractéristiques structurales des amidons natifs sur leur réactivité chimique*. PhD dissertation. France: University of Nantes.
- Imberty, A., Buléon, A., Tran, V., & Perez, S. (1991). Recent advances in knowledge of starch structure. *Starch/Stärke*, 43, 375–384.
- Jayakody, L., & Hoover, R. (2008). Effect of annealing on the structure and physico-chemical properties of starches from different botanical origins: A review. *Carbohydrate Polymers*, 74, 691–703.
- Ji, Y., Ao, Z., Han, J.-A., Jane, J.-L., & BeMiller, J. N. (2004). Waxy maize starch subpopulations with different gelatinization temperatures. *Carbohydrate Polymers*, 57, 177–190.
- Ji, N., Li, X., Qiu, C., Li, G., Sun, Q., & Xiong, L. (2015). Effects of heat moisture treatment on the physicochemical properties of starch nanoparticles. *Carbohydrate Polymers*, 117, 605–609.
- Kong, X., Sun, X., Xu, F., Umemoto, T., Chen, H., & Bao, T. (2014). Morphological and physicochemical properties of two starch mutants induced from a high amylose indica rice by gamma irradiation. *Starch-Stärke*, 66(1–2), 157–165.
- Kulp, K., & Lorenz, K. (1981). Heat-moisture treatment of starches: I-Physicochemical properties. *Cereal Chemistry*, 58, 46–48.
- Larsson, K. (1980). Inhibition of starch gelatinization by amylose-lipid complex formation. *Starch/Stärke*, 32, 125–126.
- Le Bail, P., Bizot, H., Ollivon, M., Keller, G., Bourgaux, C., & Buléon, A. (1999). Monitoring the crystallization of amylose-lipid complexes during maize starch melting using synchrotron X-ray diffraction. *Biopolymers*, 50, 99–110.
- Lim, S. T., Chang, E. H., & Chung, H. J. (2001). Thermal transition characteristics of heat/moisture treated corn and potato starches. *Carbohydrate Polymers*, 46, 107–115.
- Loisel, C., Maache-Rezzoug, Z., & Esneault, C. (2006). Effect of hydrothermal treatment on the physical and rheological properties of maize starches. *Journal of Food Engineering*, 73, 45–543.
- Maache-Rezzoug, Z., Zarguili, I., Loisel, C., Queveau, D., & Buleón, A. (2008). Structural modifications and thermal transitions of standard maize starch after D.I.C. hydrothermal treatment. *Carbohydrate Polymers*, 74(4), 802–812.
- Maache-Rezzoug, Z., Zarguili, I., Loisel, C., & Doublier, J.-L. (2010). Study of DIC hydrothermal treatment effect on rheological properties of standard maize (SMS), waxy maize (WMS), wheat (WTS) and potato (PTS) starches. *Journal of Food Engineering*, 99(4), 452–458.
- Maache-Rezzoug, Z., Zarguili, I., Loisel, C., Doublier, J.-L., & Buleón, A. (2011). Investigation on structural and physicochemical modifications of standard maize, waxy maize, wheat and potato starches after DIC treatment. *Carbohydrate Polymers*, 86(1), 328–336.
- Malumba, P., Massaux, C., Deroanne, C., Masimango, T., & Bera, F. (2009). Influence of drying temperature on functional properties of wet-milled starch granules. *Carbohydrate Polymers*, 75, 299–306.
- Maruta, I., Kurahashi, Y., Takayano, R., Hayashi, K., Yoshino, Z., Komaki, T., et al. (1994). Reduced-pressure heat-moisture treatment: A new method for heat-moisture treatment of starch. *Starch/Stärke*, 46, 177–181.
- Morrison, W. R., Tester, R. F., Snape, C. E., Law, R., & Gidley, M. J. (1993). Swelling and gelatinization of cereal starches: IV. Some effects of lipid-complexed amylose and free amylose in waxy and normal barley starches. *Cereal Chemistry*, 70, 385–391.
- Rezzoug, S. A., Maache-Rezzoug, Z., Mazoyer, J., & Allaf, K. (2000). Effect of instantaneous controlled decompression process on hydration capacity of scleroglucan: Optimisation of operating conditions by response surface methodology. *Carbohydrate Polymers*, 42, 73–84.
- Sair, L., & Fetzer, W. R. (1944). Water sorption by starches: Water sorption corn starch and commercial modifications of starches. *Industrial and Engineering Chemistry*, 36, 205–208.
- Sui, Z., Yao, T., Zhao, Y., Ye, X., Kong, X., & Ai, L. (2015). Effects of heat-moisture treatment reaction conditions on the physicochemical and structural properties of maize starch: Moisture and length of heating. *Food Chemistry*, 173, 1125–1132.
- Takaya, C. S., & Nishinari, K. (2000). Thermal studies on the gelatinisation and retrogradation of heat-moisture treated starch. *Carbohydrate Polymers*, 41, 97–100.
- Tufvesson, F., Wahlgren, M., & Eliasson, A.-C. (2003). Formation of amylose-lipide complexes and effects of temperature treatment Part 2. fatty acids. *Starch/Stärke*, 55, 138–149.
- Vermeylen, R., Goderis, B., Reynaers, H., & Delcour, J. A. (2006). Amylopectin molecular structure reflected in macromolecular organization of granular starch. *Biomacromolecules*, 7, 2624–2630.
- Wakelin, J. H., Virgin, H. S., & Crystal, E. (1959). Development and comparison of two X-ray methods for determining the crystallinity of cotton cellulose. *Journal of Applied Physics*, 30, 1654–1662.
- Wang, H., Zhang, B., Chen, L., & Li, X. (2016). Understanding the structure and digestibility of heat-moisture treated starch. *International Journal of Biological Macromolecules*, 88, 1–8.
- Zarguili, I., Maache-Rezzoug, Z., Loisel, C., & Doublier, J.-L. (2006). Influence of DIC hydrothermal process conditions on the gelatinization properties of standard maize starch. *Journal of Food Engineering*, 77(3), 454–461.
- Zarguili, I., Maache-Rezzoug, Z., Loisel, C., & Doublier, J.-L. (2009). A mathematical model to describe the change of moisture distribution in maize starch during DIC Hydrothermal treatment. *International Journal of Food Science and Technology*, 44(1), 10–17.
- Zen, F., Ma, F., Kong, F., Gao, Q., & Yu, S. (2015). Physicochemical properties and digestibility of hydrothermally treated waxy rice starch. *Food Chemistry*, 172, 92–98.